

Evaporation of single liquid drops in an immiscible liquid at elevated pressures: experimental study with n-pentane and R 113 drops in water

YASUSHI SHIMIZU and YASUHIKO H. MORI

Department of Mechanical Engineering, Keio University, 3-14-1 Hiyoshi, Kohoku-ku, Yokohama 223, Japan

(Received 19 October 1987 and in final form 16 February 1988)

Abstract—This study deals with direct contact evaporation of single liquid drops in a stagnant medium of an immiscible liquid under moderately elevated pressures. Experiments have been performed with n-pentane and R 113 drops injected into water under pressures of up to 0.48 MPa. Data obtained have been processed to yield information on parameters of practical importance: the medium height required for complete evaporation of each drop and the instantaneous heat transfer coefficient for which simple correlations are established. Particular attention has been paid to the apparent dependencies of these parameters on the nominal temperature difference as well as on the pressure.

1. INTRODUCTION

EVAPORATION of liquid drops released into a pool of an immiscible, less volatile, hotter liquid has been a subject of research motivated by various industrial needs. Development of direct-contact boilers for energy recovery from geothermal brine or industrial waste water is a current example. Freeze desalination and latent-heat cool-energy storage are other examples in which evaporation of one substance and crystallization of another simultaneously proceed. A number of studies, both theoretical and experimental, have been reported on the heat transfer aspect of the drop evaporation process. Some of these studies deal with single, isolated drops each evaporating in the course of free rise in a stagnant medium. The primary objective of these single drop studies is, we believe, to clarify the physical nature of the phenomenon and/or to establish a theoretical or empirical expression for the instantaneous or time-averaged heat transfer coefficient to be utilized in preparing a mathematical scheme for predicting multi-drop evaporation in various conditions and designing evaporators. At present no theory is available, in our opinion, that represents the actual evaporation process well and gives a reliable prediction of heat transfer to evaporating drops. Thus we must rely on experimentally-obtained knowledge and, if necessary, find out correlations for the heat transfer coefficient based on experimental data. Battya *et al.* [1], for example, reported on a regression analysis of Sideman and Taitel's data [2] to establish a correlation for the instantaneous heat transfer coefficient.

A mass of experimental data has been accumulated so far on evaporation of single drops of some volatile

oily liquid in water or some aqueous solutions [2-10]. A problem to be noted here is that all of these data are on drop evaporation under atmospheric pressure. Hence there is no evidence that the correlations established on the basis of those data are still valid, with a reasonably good approximation, at higher pressures. The dynamics of evaporating drops—each taking the form of a 'two-phase bubble' consisting of a vapor phase and an unvaporized-liquid phase—should change with pressure. The effect of the partial pressure of the continuous-phase substance in the vapor phase upon the effective temperature driving force may become more prominent, as the pressure and, accordingly, the saturation temperature are increased in a system involving a particular combination of fluid substances. The surface and interfacial tensions, which may affect the three-phase interaction, should also change with pressure and temperature. Thus it is necessary to have experimental data on drop evaporation at pressures elevated to such levels that we may encounter in direct contactors in practical use. As already reported in a separate paper [11], we designed and constructed an experimental apparatus which enables single drop evaporation at elevated pressures to be investigated. The apparatus has been used, in the present study, to investigate the evaporation of drops of n-pentane and R 113 (trichlorotrifluoroethane) in a medium of water under pressures of up to 0.48 MPa. The results obtained are presented in this paper in terms of parameters of practical importance such as the medium height required for complete evaporation of each drop and the instantaneous heat transfer coefficient. Particular attention is paid to the dependencies of those parameters on the pressure and the nominal temperature difference.

NOMENCLATURE

C	constant defined by equation (3)	T_s	temperature at which the sum of the saturated vapor pressures of the dispersed- and the continuous-phase fluids is equal to P_∞
c_p	specific heat capacity of the continuous-phase liquid	ΔT	temperature difference, ΔT_1 or ΔT_2
D	equivalent spherical diameter of two-phase bubble, $(6V/\pi)^{1/3}$	ΔT_1	$T_\infty - T_{1s}$
h	instantaneous heat transfer coefficient based on equivalent spherical surface area of two-phase bubble	ΔT_2	$T_\infty - T_s$
H	vertical position of two-phase bubble measured from the nozzle tip	U, \bar{U}	instantaneous and average rise velocities of two-phase bubble, respectively
H_v	H at which evaporation is complete	V	volume of two-phase bubble.
Δh_v	specific latent heat of vaporization of the dispersed-phase liquid	Greek symbols	
Ja	Jakob number, $\rho c_p \Delta T / (\rho_v \Delta h_v)$	α	thermal diffusivity of the continuous-phase liquid
k	thermal conductivity of the continuous-phase liquid	ξ	vapor mass ratio in two-phase bubble
Nu	Nusselt number, hD/k	ρ, ρ_v	mass densities of the continuous-phase liquid and of the vapor, respectively.
P_∞	local pressure	Subscripts	
P^*	P_∞ at nozzle outlet	0	initial value
P_{1s}, P_{2s}	saturated vapor pressures of the dispersed- and the continuous-phase fluids, respectively	1	related to ΔT_1
Pe	Peclet number, UD/α	2	related to ΔT_2 .
\dot{Q}	rate of heat flow into the two-phase bubble	Superscript	
t_v	time required for complete evaporation	*	at nozzle outlet.
T_{1s}	saturation temperature of the dispersed-phase fluid corresponding to P_∞		

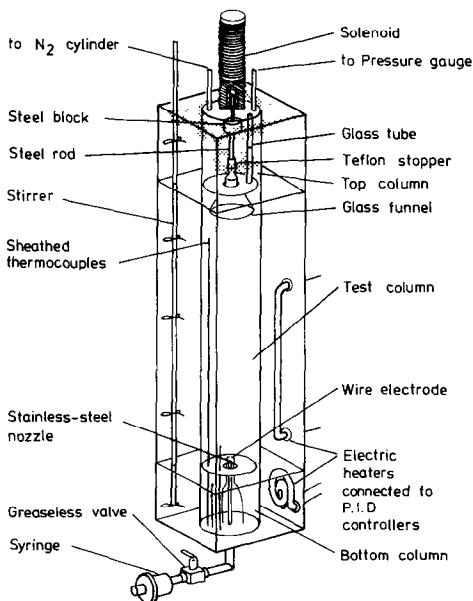


FIG. 1. Schematic diagram of the experimental apparatus.

2. EXPERIMENTS

2.1. Scheme of experiments

The experimental setup used in the present study essentially consisted of the main portion illustrated in Fig. 1 and some auxiliary devices for photography.

Since the details of the main portion are given in a preceding paper [11], we describe its structure only briefly here. It consisted of two vertically-oriented concentric columns—the inner one circular of 77 mm i.d., and the outer square in cross section—both made of transparent polycarbonate. The columns were each partitioned into three parts, by setting baffle plates at two particular elevations. For brevity we call hereafter the three parts of the inner column 'the bottom column', 'the test column' and 'the top column', respectively, in an ascending scale. The whole space in the bottom and the test columns plus a small part of the top column were filled with distilled water, while the rest of the space in the top column was filled with an externally-supplied pressure-regulated nitrogen gas. The three parts of the outer column served as water baths the temperatures of which were controlled independently. These baths made it possible to set the temperature in the test column at a desired level while maintaining the temperatures in the bottom and the top columns at lower than and nearly equal to the saturation temperature, respectively, of n-pentane or R 113 which was used as the volatile liquid to form drops in the test column.

Before each experimental run the test section was sealed against the top column, using a specially-designed solenoid valve, except at the opening of a dilatometer tube which stood in the top column. The

volatile liquid, n-pentane or R 113 in the liquid state, contained in a high-pressure syringe located outside the column assembly was displaced through a tubular nozzle, which passed through the bottom column and protruded out of the test column, to form a drop perching at the outlet of the nozzle. The run was started by triggering a nucleation in the drop with the aid of an electric discharge between wire electrodes installed just above the drop. The drop was released from the nozzle outlet immediately after the discharge, and rose in the test column taking the form of a two-phase bubble. The two-phase bubble in the course of the rise was photographed by a 35 mm motor-driven camera which was set on a slide stand. Simultaneously the meniscus in ascending motion in the dilatometer tube was photographically recorded, with exposure signals sent from the 35 mm camera, using a Locam Model 51 16 mm cinecamera. The photographs obtained were used to find the changes with time in the vertical position and in the volume of each two-phase bubble and thereby to yield the rise velocity of and the rate of heat flow into the bubble.

2.2. Fluid samples

Water used as the medium liquid was taken from a commercial purification apparatus which comprised a reverse-osmosis device and an ion-exchange device as well as an all-glass distillation unit. n-Pentane and R 113 were of 99.0 and 99.9% wt certified purities, respectively. They were used as received from their manufacturers.

Before feeding these fluids into the inner column and the syringe to prepare for each series of experiments, we disassembled them, cleaned their components using almost the same process as that of Nosoko *et al.* [12] in cleaning the components of their evaporation chamber, and then assembled them again carefully to prevent their inside surfaces from being contaminated with human skin oil. Thus we presume that the test fluids in place were not contaminated compared to the same fluids before use.

2.3. Definitions of reference pressure and temperature difference

The local pressure in the test column, P_∞ , is given by adding the hydrostatic head at the location of interest to the pressure measured in the top column. The local pressure at the depth of the nozzle outlet is distinguished as P^* , which is used to indicate the degree of pressurization in each run.

Defining the temperature difference is a somewhat annoying problem, because the temperature at the evaporating surface of the volatile liquid in each two-phase bubble can vary time to time and place to place depending on the partial pressure of the water vapor possibly in contact with the surface. The possible upper and lower limits of the temperature are given respectively by the saturation temperature T_{1s} of the volatile liquid under the local pressure P_∞ and by a temperature T_s at which the sum of saturated vapor

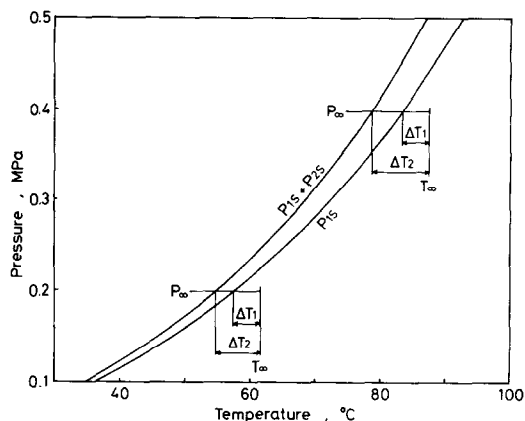


FIG. 2. Variations of saturated vapor pressures of n-pentane, P_{1s} , and the sum of saturated vapor pressures of n-pentane and water, $P_{1s} + P_{2s}$, with temperature. ΔT_1 and ΔT_2 are indicated at two levels of system pressure P_∞ , assuming, as an illustrative example, that $\Delta T_1 = 4$ K.

pressure of the volatile liquid, P_{1s} , and that of water, P_{2s} , is equal to P_∞ . Thus, we define two limiting temperature differences: $\Delta T_1 \equiv T_\infty - T_{1s}$ and $\Delta T_2 \equiv T_\infty - T_s$, where T_∞ denotes the undisturbed water temperature measured using thermocouples in the test column. In the course of rise of each two-phase bubble, ΔT_1 and ΔT_2 increase with a decrease in the hydrostatic head. The extent of their increases over the whole height of the test column (650 mm) is a little over 1 K. The values of ΔT_1 and ΔT_2 corresponding to the pressure P^* are denoted by ΔT_1^* and ΔT_2^* , respectively, and are used as a duplex measure of the degree of temperature difference in each run.

Figure 2 illustrates, for the case of the n-pentane/water system, the variations of P_{1s} and $P_{1s} + P_{2s}$ with temperature, and the variations of ΔT_1 and ΔT_2 with pressure P_∞ . It should be noted that the discrepancy between ΔT_1 and ΔT_2 increases with an increase in P_∞ .

3. RESULTS AND DISCUSSION

3.1. Rise motion of two-phase bubbles

The dynamic behavior of evaporating two-phase bubbles was apparently the same throughout the present experiments. Both n-pentane and R 113 bubbles showed some shape oscillation and a wobbling in trajectory in the course of rise even at the highest pressure which was close to 0.5 MPa in the case of n-pentane bubbles and 0.4 MPa in the case of R 113 bubbles.

Photographic records of bubbles showed that the vertical position H of each bubble changed almost linearly with time in each evaporation process [11]. By fitting a cubic function of time to the data on the position vs time relation for each bubble and by differentiating the function with respect to time, we have obtained the instantaneous rise velocity U of the bubble as a function of time. At the same time we have obtained, as will be explained later, the equivalent

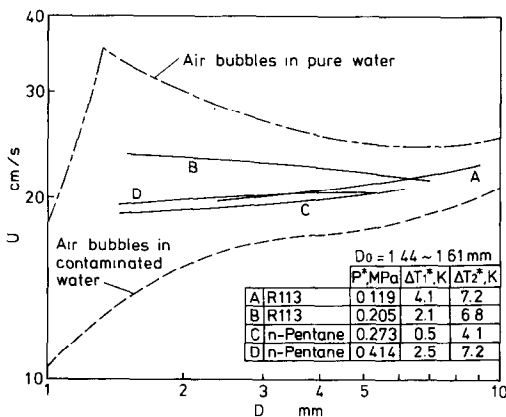


FIG. 3. Instantaneous rise velocity of two-phase bubbles plotted against their instantaneous diameters. Standard curves for terminal velocities of air bubbles in pure water and in surfactant-contaminated water [13] are also shown for comparison.

spherical diameter D of the bubble as a function of time based on the dilatometric record. Combining these results we obtain the U vs D relation for each bubble in the course of its growth. Some typical examples are shown in Fig. 3. It is seen that U is nearly constant throughout each evaporation process and is little dependent on the pressure as well as on the substance forming the bubble. If we define the average velocity \bar{U} of a bubble as the quotient of its vertical displacement H , till the completion of evaporation by the time lapse t_v after its release from the nozzle till the completion of evaporation, and sum up all the experimental results, we see that $\bar{U} = 203 \pm 35$ mm s⁻¹. In a model calculation presented later we assume that the instantaneous velocity U is held at 203 mm s⁻¹ throughout each evaporation process.

Also shown in Fig. 3 for comparison are curves representing two extremes of terminal velocities of air bubbles in water: one is for air bubbles in highly purified water and the other for air bubbles in surfactant-contaminated water [13]. Apparently the velocities of our two-phase bubbles are at intermediate levels between the extremes. If we take into account the fact that the two-phase bubbles suffered some reduction of buoyancy because of the mass of unvaporized liquid involved, we see that their rise motion is effectively closer to that for highly purified systems. This may be ascribed in part to the two-phase bubble surface being deficient in adsorbed molecules of surfactant contaminants because of its expansion, and hence being sufficiently mobile. We do not dare to speculate further on this aspect of the phenomenon in this paper.

3.2. Dilatometric records of two-phase bubble growth

Figure 4 exemplifies dilatometrically-obtained data on the change in volume of each two-phase bubble, $V - V_0$, for four runs selected arbitrarily. Note that in two of the runs ΔT_1 was negative over the whole evaporation process or at least a major part of the

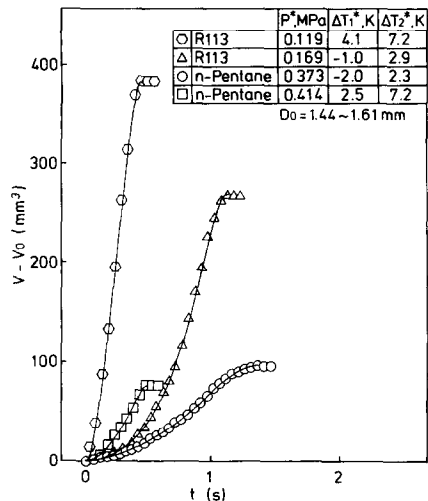


FIG. 4. Dilatometrically-obtained data (open symbols) on the change in volume of two-phase bubbles and cubic curves fitted to the data.

evaporation process. The evaporation can proceed irrespective of the sign of ΔT_1 whenever ΔT_2 is positive. It is seen in Fig. 4 that $V - V_0$ sharply levels off as the evaporation is completed in each run. Thus we can accurately determine the evaporation time t_v on each dilatometric record, and then determine, by comparing it with the H vs t relation, the evaporation height H_v . We have found that the variation of $V - V_0$ with t in each run can be approximated well by joining two different cubic functions of time, each covering the earlier or the later part of the evaporation process. The solid curve laid over each set of data points in Fig. 4 represents a pair of cubic functions which have been so determined, using the method of least squares, that they have a common first derivative at an intermediate stage of the evaporation process where they are joined. The agreement between such a fitted curve and the data points is satisfactory in every run. Since the value of V_0 , which is to be added to $V - V_0$ to give the instantaneous two-phase bubble volume V , can readily be calculated based on the final value of $V - V_0$, we get a functional expression for V for each run. The expression permits us to deduce the D vs t relation and, by differentiating with respect to time, the heat flow rate and the heat transfer coefficient as functions of time.

3.3. Evaporation height

The evaporation height H_v is a parameter having a direct influence on the required size of evaporators. Its dependencies on the pressure and the temperature difference are presented below.

Figures 5(a) and (b) show the data on H_v plotted against P^* . On the graphs on the left-hand side the data are grouped into four to five classes on the basis of ΔT_1^* . On the graphs on the right-hand side the same is done but on the basis of ΔT_2^* . As for the

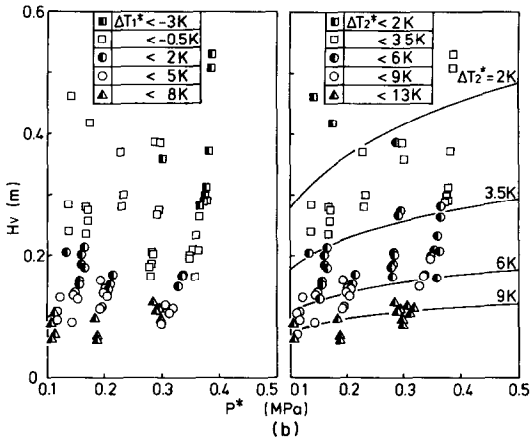
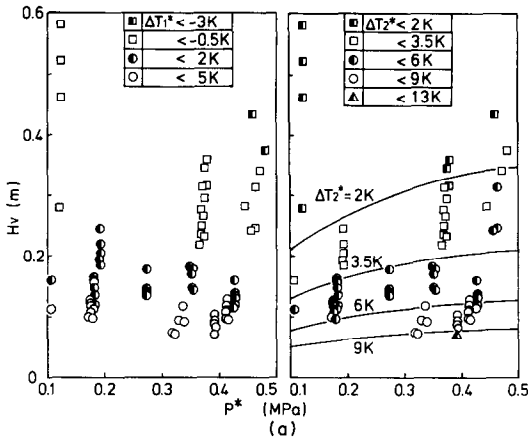


FIG. 5. Pressure dependency of the height, above the nozzle outlet, where evaporation is complete. Data are grouped into four or five classes on the basis of ΔT_1^* or ΔT_2^* serving as the parameter. Curves represent predictions obtained by substituting $U = 203 \text{ mm s}^{-1}$ into equation (4a) or (4b): (a) n-pentane/water; (b) R 113/water.

curves drawn on the graphs on the right-hand side an explanation is given in the following section.

Comparing Figs. 5(a) and (b), we recognize that R 113 bubbles generally cover longer vertical distances till the completion of evaporation than n-pentane bubbles do. Since there is little difference, between n-pentane and R 113 bubbles, both in surface area and in rise velocity, the appreciable difference in H_v should be related to the difference in the heat transfer coefficient which is shown later.

The apparent dependency of H_v on P^* is somewhat confusing. The graphs on the left-hand side in Figs. 5(a) and (b) show that H_v tends to decrease with P^* when ΔT_1^* is held constant at a relatively low level. The tendency must result from the 'effective' temperature difference increasing with P^* , because of an increasing effect of water-vapor pressure, while ΔT_1^* is held constant. The lower the value of ΔT_1^* , the wider the relative discrepancy between the 'effective' temperature difference and ΔT_1^* . On the graphs on the right-hand side we note, on the contrary, that H_v increases with an increasing P^* at each level of ΔT_2^* .

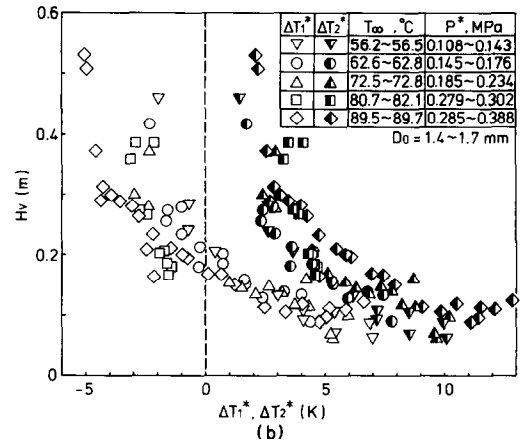
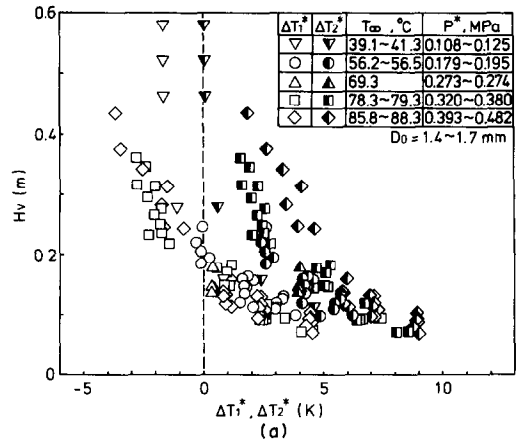


FIG. 6. Temperature-difference dependency of the height, above the nozzle outlet, where evaporation is complete: (a) n-pentane/water; (b) R 113/water.

This tendency may be exaggerated to some extent because of the 'effective' temperature difference decreasing possibly with P^* while ΔT_2^* is held constant. Nevertheless, the above tendency seems reasonable, at least qualitatively speaking, because an increase in P^* (or P_{∞}) causes a reduction in the bubble surface area, which in turn can suppress the rate of heat flow into each bubble.

In Figs. 6(a) and (b) the H_v data are plotted against ΔT_1^* and ΔT_2^* simultaneously. It is seen that H_v increases enormously as ΔT_2^* almost vanishes. (The critical condition for no evaporation is given not by vanishing ΔT_2^* but by vanishing ΔT_2 at the top of the test column.) Also recognized in each of these figures is the discrepancy between the H_v vs ΔT_1^* relation and the H_v vs ΔT_2^* relation increasing with an increase in P^* or T_{∞} . When ΔT_2^* (or, to be more general, ΔT_2) is as low as a few degrees or less, ΔT_1^* (or ΔT_1) almost vanishes or even becomes negative, even at the lowest level of P^* , and loses its normal meaning as the temperature driving force.

3.4. Heat transfer characteristics

The instantaneous rate of heat flow into each two-phase bubble, \dot{Q} , has been deduced from the dV/dt vs

t relation and a simple assumption on the thermodynamic state in the bubble. One possible assumption is to suppose that the bubble consists of saturated liquid and saturated vapor of *n*-pentane or R 113 corresponding to the local pressure P_∞ . Another one is to suppose that the bubble consists of saturated liquid of *n*-pentane or R 113 and saturated common vapors of *n*-pentane or R 113 and water. The values of \dot{Q} predicted from the latter assumption are higher than the corresponding values predicted from the former assumption by 4–10% in the case of *n*-pentane bubbles and 9–12% in the case of R 113 bubbles. The latter assumption also provides the maximum evaluation of the fraction of \dot{Q} used for evaporating water, which is 9–18% in the case of *n*-pentane bubbles and 20–23% in the case of R 113 bubbles. Here we use rather arbitrarily the former assumption to evaluate \dot{Q} and thereby the instantaneous heat transfer coefficient which is defined in two ways as

$$h_1 = \dot{Q}/(\pi D^2 \Delta T_1), \quad h_2 = \dot{Q}/(\pi D^2 \Delta T_2).$$

It is a matter of controversial opinion how to assume a dimensionless correlation for expressing h_1 or h_2 . Sideman and Isenberg [14], for example, proposed the following semi-empirical correlation partly based on experimental results obtained by Sideman and Taitel [2]:

$$Nu_1 = 0.272 Pe^{1/2} \quad (1)$$

where physical properties of the continuous-phase liquid are used in the h_1 -based Nusselt number Nu_1 † and in Peclet number Pe . More recently Battya *et al.* [1] assumed, also based on the experimental results of Sideman and Taitel, the following correlation:

$$Nu_1 = 0.64 Pe^{0.5} Ja^{-0.35}. \quad (2)$$

These correlations are based on such a view that the thermal resistance of the unvaporized liquid in each two-phase bubble can be neglected compared to that of the continuous phase. The lead constants in these correlations are significantly lower than those given in the corresponding correlations for continuous-phase-side heat transfer to or from isothermal fluid spheres [16]. This fact is ascribable, according to the above view, to a reduction of the effective heat-transfer surface area due to a fractional occupation of the bubble surface by a nearly-insulating vapor phase. Although there is some doubt concerning the validity of the above view [4, 5], we follow it in presenting our experimental results.

† Sideman and Taitel [2] wrote that they defined the temperature difference, in evaluating the heat transfer coefficient, as an excess of T_∞ over the average of ‘boiling points’ of the dispersed-phase liquid at the top and the bottom of their test column. According to Taitel [15] the ‘boiling points’ mean T_{1s} ’s at respective locations. Thus the heat transfer coefficient that they used almost corresponds to h_1 , and hence the Nusselt number used in Sideman and Isenberg’s correlation can well be regarded as the h_1 -based Nusselt number.

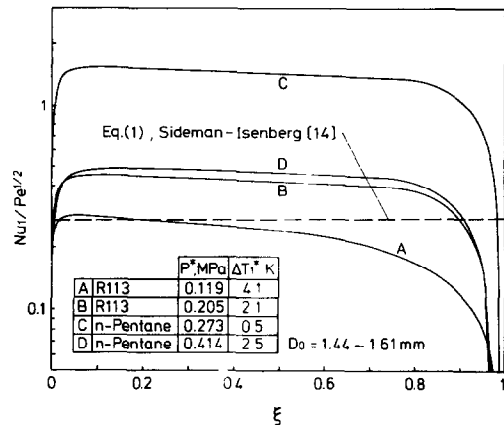


FIG. 7. Typical examples of variation of $Nu_1/Pe^{1/2}$ with vapor mass ratio. Each of the runs identified as A, B, C and D is the same run as that exemplified in Fig. 3 with the same notation.

Figure 7 shows the variation of $Nu_1/Pe^{1/2}$ with the vapor mass ratio ξ in each of the same four runs that are exemplified in Fig. 3. It is recognized that $Nu_1/Pe^{1/2}$ has an approximately constant value over the major part of the whole range of ξ in each run. This is just the case when Nu_1 is replaced by the h_2 -based Nusselt number Nu_2 . This fact seems to justify assuming, as the first approximation, that $Nu/Pe^{1/2}$ ($Nu_1/Pe^{1/2}$ or $Nu_2/Pe^{1/2}$) has a constant value throughout each entire evaporation process. We have so determined the constant value, C , that the same evaporation time t_e as the one actually measured is predictable from the assumption that $Nu/Pe^{1/2}$ is held at C throughout the evaporation process. That is

$$C = \int_0^{t_e} D Nu \Delta T dt / \int_0^{t_e} D Pe^{1/2} \Delta T dt \quad (3)$$

where ΔT should read ΔT_1 or ΔT_2 , and Nu should read Nu_1 or Nu_2 . Plotted against ΔT_1^* and ΔT_2^* in Figs. 8(a) and (b), respectively, are such constant values. The figures show that ΔT_1 -based C tends to increase sharply with a decrease in ΔT_1^* and that the higher the level of P^* (or T_∞), the higher the value of C at each level of ΔT_1^* . Evidently these features come from the discrepancy of the ‘effective’ temperature difference from the nominal temperature difference ΔT_1 , because of finite water-vapor pressure. A pair of solid curves given in each figure shows the predictions based on equation (2), the correlation that Battya *et al.* [1] obtained by a regression analysis using Sideman and Taitel’s experimental results [2]. The correlation represents the above-mentioned dependency of ΔT_1 -based C on ΔT_1^* to some extent, and we believe, in opposition to the version offered by Battya *et al.* [17], that the temperature-difference dependency of heat transfer coefficient seen in Sideman and Taitel’s results on which the correlation is based is also related to the effect of water-vapor pressure. Based on a numerical analysis of the heat transfer to a growing bubble, Battya *et al.* [17] claimed that as the Jakob number

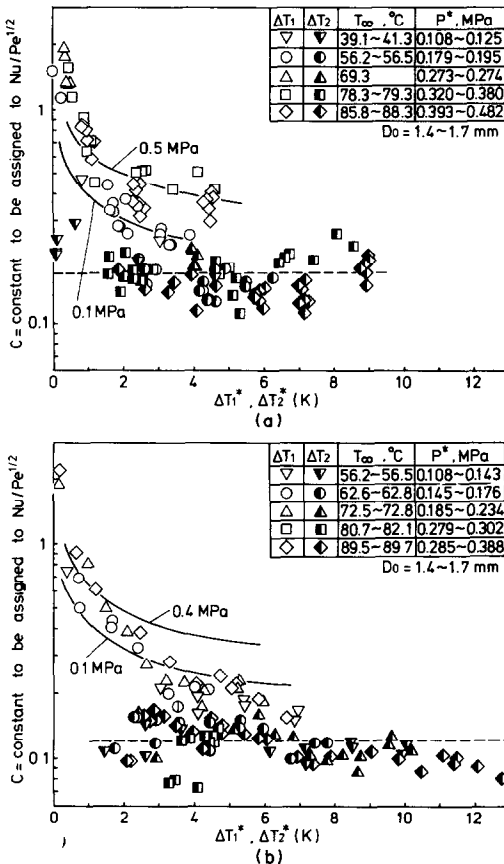


FIG. 8. Temperature-difference dependency of $Nu/Pe^{1/2}$ assumed to be constant in each evaporation process. Curves represent predictions based on equation (2), the correlation of Battya *et al.* [1]: (a) n-pentane/water; (b) R 113/water.

Ja increases, resulting in an increase in the bubble growth rate, the thermal boundary layer around a bubble thickens resulting in such a decrease in Nu as represented by the correlation. However, we do not accept their analysis as well as their version based on it. Our criticisms directed at their analysis are described elsewhere [18].

In Figs. 8(a) and (b) the data points for ΔT_2 -based C are scattered, irrespective of the level of P^* , about a certain level which seems little dependent on ΔT_2^* . This fact means that employing ΔT_2 instead of ΔT_1 is much more advantageous in characterizing the heat transfer to each two-phase bubble. The dashed horizontal line drawn in each figure shows the average of all data on ΔT_2 -based C . The average is recommended for use in formulating the Nu_2 vs Pe relation, as the lead constant; that is

$$Nu_2 = 0.169Pe^{1/2} \quad (4a)$$

for the n-pentane/water system, and

$$Nu_2 = 0.121Pe^{1/2} \quad (4b)$$

for the R 113/water system.

Combining either of the above correlations for Nu_2 and an appropriate expression for the rise velocity of

bubbles, U , we can predict the evaporation height H_v . If we assume that $U = 203 \text{ mm s}^{-1}$ and combine it respectively with those correlations, we get the predictions of H_v shown by the solid curves in Figs. 5(a) and (b). The agreement between the predictions and the data points is generally good in the case of the n-pentane/water system, but it becomes poor with an increase in ΔT_2^* in the case of the R 113/water system. The latter fact is related to an increasing deviation of respective ΔT_2 -based C values from their average with an increasing ΔT_2^* .

Throughout Figs. 5, 6 and 8 we see that the heat transfer performance in the R 113/water system is appreciably inferior to that in the n-pentane/water system. There is no significant difference in mechanical and thermal properties between n-pentane and R 113 except in density. The larger density of liquid R 113 can contribute by itself to subduing the spreading of the unvaporized liquid over the surface of each two-phase bubble, which is possibly driven by the capillary force and the sloshing motion of the unvaporized liquid itself. Unfortunately we do not have sufficient knowledge, however, on the interfacial properties as well as the dynamics of the sloshing motion in those systems. Thus we cannot evaluate to what extent the above-mentioned difference in the heat transfer performance between those two systems is ascribable to the difference in density of the dispersed-phase liquid.

4. CONCLUSIONS

We have obtained experimental results on evaporation of single n-pentane drops and R 113 drops, both from 1.4 to 1.7 mm in initial diameter, released in the medium of water under pressures of up to 0.48 and 0.39 MPa, respectively. The results giving information of, in our opinion, practical importance are summarized in Figs. 3, 5, 6 and 8. The specific points to be stressed are given below.

(1) The rise velocity of each drop taking the form of a growing two-phase bubble is held nearly constant at about 203 mm s^{-1} in the course of evaporation in the whole range of experiments.

(2) The neglect of water vapor pressure in defining the reference dispersed-phase temperature can yield an inadequate evaluation of temperature difference, which results in a peculiar superficial dependency of heat transfer characteristics on the temperature difference. Defining the temperature difference on the assumption of saturated common vapors, of n-pentane or R 113 and water, in contact with the evaporating surface in two-phase bubbles is rather recommended, because it almost eliminates the above problem and enables the heat transfer characteristics to be expressed independently of the temperature difference and of the pressure.

(3) The empirical correlations for instantaneous Nusselt number (equations (4a) and (4b)) are

proposed. They are suited, because of their simplicity, to be incorporated in various schemes of mathematical modeling of direct-contact evaporation heat transfer. Use of each correlation in combination with the assumption of constant rise velocity (203 mm s^{-1}) is recommended.

Acknowledgements—We acknowledge with thanks S. Saeki, T. Mori and T. Tezuka, former and present students at the Department of Mechanical Engineering, Keio University, for their assistance in the experimental work.

REFERENCES

1. P. Battya, V. Vijay, P. Raghavan and K. Seetharamu, Parametric studies on direct contact evaporation of a drop in an immiscible liquid, *Int. J. Heat Mass Transfer* **27**, 263–272 (1984).
2. S. Sideman and Y. Taitel, Direct-contact heat transfer with change of phase: evaporation of drops in an immiscible liquid medium, *Int. J. Heat Mass Transfer* **7**, 1273–1289 (1964).
3. D. H. Klipstein, Heat transfer to a vaporizing immiscible drop, D.Sc. thesis, Massachusetts Institute of Technology (1963).
4. C. B. Prakash and K. L. Pinder, Direct contact heat transfer between two immiscible liquids during vaporization. Part I: Measurement of heat transfer coefficient; Part II: Total evaporation time, *Can. J. Chem. Engng* **45**, 210–220 (1967).
5. A. E. S. Adams and K. L. Pinder, Average heat transfer coefficient during the direct evaporation of a liquid drop, *Can. J. Chem. Engng* **50**, 707–713 (1972).
6. H. C. Simpson, G. C. Beggs and M. Nazir, Evaporation of butane drops in brine, *Desalination* **15**, 11–23 (1974).
7. Y. Tochitani, Y. H. Mori and K. Komotori, Vaporization of single liquid drops in an immiscible liquid. Part I: Forms and motions of vaporizing drops, *Wärme- und Stoffübertr.* **10**, 51–59 (1977).
8. M. G. Ortiz M., A. Campo, V. Capozzi, D. Ochoa and M. Zinguer, Direct contact heat exchanger: an experimental study, *Proc. 7th Int. Heat Transfer Conf.*, Vol. 6, pp. 337–340. Hemisphere, Washington, DC (1982).
9. M. R. Mokhtarzadeh-Dehghan and A. A. El-Shirbini, Dynamics of and heat transfer to a butane droplet evaporating in water, *Wärme- und Stoffübertr.* **20**, 69–75 (1986).
10. W. Helmer, S. Nagarjan and M. Rane, A new method of experimentally determining heat transfer coefficients in direct-contact bubble evaporation. In *Developments in Experimental Techniques in Heat Transfer and Combustion*, ASME HTD-Vol. 71, pp. 37–43. ASME, New York (1987).
11. Y. Shimizu and Y. H. Mori, Evaporation of single liquid drops in an immiscible liquid at elevated pressures: equipment and preliminary results, *Exp. Fluids* **6**, 73–79 (1987).
12. T. Nosoko, T. Ohyama and Y. H. Mori, Evaporation of volatile-liquid lenses floating on an immiscible-liquid surface: effects of the surface age and fluid purities in n-pentane/water system, *J. Fluid Mech.* **161**, 329–346 (1985).
13. R. Clift, J. R. Grace and M. E. Weber, *Bubbles, Drops, and Particles*, pp. 171–173. Academic Press, New York (1978).
14. S. Sideman and J. Isenberg, Direct contact heat transfer with change of phase: bubble growth in three-phase systems, *Desalination* **2**, 207–214 (1967).
15. Y. Taitel, Personal communication to Y. Shimizu (1987).
16. R. Clift, J. R. Grace and M. E. Weber, *Bubbles, Drops, and Particles*, pp. 135–137. Academic Press, New York (1978).
17. P. Battya, V. R. Raghavan and K. N. Seetharamu, A theoretical correlation for the Nusselt number in direct contact evaporation of a moving drop in an immiscible liquid, *Wärme- und Stoffübertr.* **19**, 61–66 (1985).
18. Y. Shimizu and Y. H. Mori, Direct contact heat transfer to bubbles with simultaneous translation and growth, to be published.

EVAPORATION D'UNE GOUTTE LIQUIDE UNIQUE DANS UN LIQUIDE NON MISCIBLE A PRESSION ELEVEE: ETUDE EXPERIMENTALE AVEC n-PENTANE ET R 113 DANS L'EAU

Résumé—Cette étude concerne l'évaporation avec contact direct de gouttes liquides uniques dans un milieu stagnant qui est un liquide non miscible sous des pressions modérément élevées. Des expériences sont faites avec n-pentane et R 113 en gouttes injectées dans l'eau sous des pressions allant jusqu'à 0,48 MPa. Les résultats obtenus sont traités pour fournir une information sur des paramètres d'importance pratique: la hauteur du milieu nécessaire pour une évaporation complète de chaque goutte et le coefficient de transfert instantané sont précisés par des formules simples. Une attention particulière est portée à la dépendance de ces paramètres vis-à-vis de la différence nominale de température aussi bien que de la pression.

DIE VERDAMPFUNG VON EINZELNEN FLÜSSIGKEITSTROPFEN IN EINER NICHT MISCHBAREN FLÜSSIGKEIT BEI ERHÖHTEN DRÜCKEN: EXPERIMENTELLE UNTERSUCHUNG MIT TROPFEN AUS n-PENTAN UND R 113 IN WASSER

Zusammenfassung—Die vorliegende Untersuchung beschäftigt sich mit der Direkt-Kontakt-Verdampfung von einzelnen Flüssigkeitstropfen in einer ruhenden, nicht mischbaren Flüssigkeit bei mäßig erhöhten Drücken. Versuche wurden mit Tropfen aus n-Pentan und R 113 durchgeführt, die bei Drücken bis zu 0,48 MPa in Wasser eingespritzt wurden. Die so gewonnenen Daten wurden ausgewertet, so daß sich Informationen über praktisch wichtige Parameter ergaben: die zur vollständigen Verdampfung jedes Tropfens benötigte Flüssigkeitshöhe und der momentane Wärmeübergangskoeffizient, für den einfache Korrelationen aufgestellt wurden. Besonderes Augenmerk wurde auf die Abhängigkeit dieser Parameter von der tatsächlichen Temperaturdifferenz und vom Druck gelegt.

**ИСПАРЕНИЕ ЕДИНИЧНЫХ КАПЕЛЬ ЖИДКОСТИ В ДРУГОЙ НЕСМЕШИВАЮЩЕЙСЯ
ЖИДКОСТИ ПРИ ПОВЫШЕННЫХ ДАВЛЕНИЯХ: ЭКСПЕРИМЕНТАЛЬНОЕ
ИССЛЕДОВАНИЕ ИСПАРЕНИЯ КАПЕЛЬ n-ПЕНТАНА И ФРЕОНА-113 В ВОДЕ**

Аннотация—Исследуется непосредственное контактное испарение единичных капель жидкости в неподвижной среде другой несмешивающейся жидкости при повышенных давлениях. Эксперименты проводились с каплями n-пентана и фреона-113, вводимых в воду при давлениях, не превышающих 0,48 МПа. Обработка экспериментальных данных позволила получить информацию о таких практически важных параметрах как толщина слоя жидкости, необходимая для полного испарения каждой капли, и текущее значение коэффициента теплообмена, для которого имеются простые обобщающие соотношения. Особое внимание обращено на явную зависимость этих параметров от номинальной разности температур и от давления.